



HHS Public Access

Author manuscript

Nat Chem Biol. Author manuscript; available in PMC 2013 May 01.

Published in final edited form as:

Nat Chem Biol. 2012 November ; 8(11): 887–889. doi:10.1038/nchembio.1065.

Enzyme Redesign Guided by Cancer-Derived *IDH1* Mutations

Zachary J. Reitman¹, Bryan D. Choi¹, Ivan Spasojevic², Darell D. Bigner¹, John H. Sampson¹, and Hai Yan^{1,*}

¹The Department of Pathology, Duke University Medical Center, Durham, North Carolina, United States of America

²The Clinical Pharmacology Lab, Duke Cancer Institute and Department of Medicine/Oncology, Duke University Medical Center, Durham, North Carolina, United States of America

Abstract

Mutations in an enzyme can result in a neomorphic catalytic activity in cancers. We applied cancer-associated mutations from isocitrate dehydrogenases (IDHs) to homologous residues in the active sites of homoisocitrate dehydrogenases (HIDHs) to derive enzymes that catalyze the conversion of 2-oxoadipate to (*R*)-2-hydroxyadipate, a critical step for adipic acid production. Thus, we provide a prototypic example of how insights from cancer genome sequencing and functional studies can aid in enzyme redesign.

Keywords

IDH1; IDH2; enzyme design; β -hydroxyacid α -decarboxylase; β -hydroxyacid oxidative decarboxylase; R132H; (*R*)-2-hydroxyadipate dehydrogenase

New organic synthesis techniques and metabolic engineering methods often rely on the generation of enzymes with novel catalytic activities. Cancer is a process of microevolution that selects for functional alterations that benefit tumor cells, including gain-of-function mutations in metabolic enzymes¹. Cancer mutational data therefore represents an until-now unappreciated source of enzyme functional diversity, which is becoming increasingly accessible as cancer sequencing data increases logarithmically with improvements in sequencing technology and as cancer geneticists turn their attention to cellular metabolic enzymes. We hypothesized that insights from mutated enzymes in cancer could guide the

Users may view, print, copy, download and text and data- mine the content in such documents, for the purposes of academic research, subject always to the full Conditions of use: http://www.nature.com/authors/editorial_policies/license.html#terms

*To whom correspondence should be addressed. hai.yan@dm.duke.edu (H.Y.).

Competing financial interests

The authors are listed on a patent that is pending related to the mutated enzymes discussed in the text. This intellectual property is managed by Duke University.

Author contributions

Z.J.R. and B.D.C., performed experiments and wrote the manuscript; I.S., performed LC-MS/MS analysis; D.D.B. and J.H.S., provided reagents; H.Y., contributed reagents, funding, and critical feedback on the manuscript.

Additional information

Supplementary information is available online at <http://www.nature.com/naturechemicalbiology/>. Reprints and permissions information is available online at <http://www.nature.com/reprints/index.html>. Correspondence and requests for materials should be addressed to H.Y.

redesign of a useful enzyme. To demonstrate this approach, we applied insights from cancer mutations to derive an enzyme that overcomes a hurdle to the clean, bio-based production of adipic acid.

Adipic acid ($\text{HOOC}(\text{CH}_2)_4\text{COOH}$, 1,4-butanedicarboxylic acid) is a substrate for the synthesis of nylon-6,6, and is one of the most-produced chemicals worldwide. There is great interest in developing biological methods for adipic acid synthesis to lower the cost of input materials, to obviate the need for fossil fuel substrates, and to reduce the release of pollutants compared to standard catalytic methods of synthesis²⁻⁴. Multiple enzymatic transformations that would support one proposed fully biological method⁵ have recently become technically possible⁶. However, the enzymatic conversion of 2-oxoadipate to (*R*)-2-hydroxyadipate, a key step in the proposed pathway, remains a major challenge⁶.

To engineer an enzyme to catalyze the conversion of 2-oxoadipate to (*R*)-2-hydroxyadipate, termed an (*R*)-2-hydroxyadipate dehydrogenase, we used insights from gain-of-function IDH mutants found in human cancer. IDHs are ubiquitous throughout life and convert (*2R*, *3S*)-isocitrate to 2-oxoglutarate, which is also known as α -ketoglutarate⁷ (Fig. 1a). All IDHs belong to the enzyme subfamily of metal ion-dependent pyridine-dinucleotide-linked β -hydroxyacid oxidative decarboxylases that act on substrates with the (*R*) configuration at the C-2 position⁸ (hereafter, β -hydroxyacid oxidative decarboxylases). HIDHs belong to the same β -hydroxyacid oxidative decarboxylase subfamily as the IDHs, but the HIDHs instead convert (*2R*, *3S*)-homoisocitrate, a 6-carbon-backbone analog of (*2R*, *3S*)-isocitrate, to 2-oxoadipate in yeast, thermophilic bacteria, and archaea⁸⁻¹³ (Fig. 1b). Recent exome sequencing revealed that missense mutations in NADP⁺-dependent IDHs, IDH1 and IDH2, occur frequently in the somatic cells of gliomas and other cancers^{14, 15}. The IDH mutations alter active site residues that contact the β -carboxyl of (*2R*, *3S*)-isocitrate, including Arg132 of IDH1, Arg140 of IDH2, and Arg172 of IDH2^{16, 17}. These mutations cause the IDH enzymes to lose their native oxidative decarboxylase activity and gain a simple oxidoreductase activity to convert 2-oxoglutarate to (*R*)-2-hydroxyglutarate^{1, 17} (Fig. 1c). Our goal was to generate a similar oxidoreductase that favored substrates with a 6-carbon backbone. IDH cancer mutants have this desired simple oxidoreductase activity but favor substrates with a 5-carbon backbone, whereas wild-type HIDHs do not have this activity yet act on substrates with a 6-carbon backbone. Here, we applied mutations homologous to those observed in IDHs in cancer to HIDHs to generate a simple oxidoreductase function to convert 2-oxoadipate to (*R*)-2-hydroxyadipate⁶, *i.e.*, the desired (*R*)-2-hydroxyadipate dehydrogenase (Fig. 1d).

To identify HIDH residues homologous to IDH cancer mutation hotspots, we compared the substrate-bound active site structures of human cytoplasmic NADP⁺-dependent isocitrate dehydrogenase (*Hs*IDH1)¹⁸ and *Schizosaccharomyces pombe* (*Sp*) HIDH¹⁹ (Fig 2a). Overlay analysis revealed that the critical substrate-binding residues Arg100 and Arg132 contained within α -helix 5 and β -strand 5 of *Hs*IDH1, respectively, were conserved in relative topography to Arg97 and Arg126 of *Sp*HIDH. The structural homology between *Hs*IDH1 and *Sp*HIDH was used as an anchor to align their primary protein sequences with each other, and also to the greater family of β -hydroxyacid oxidative decarboxylases, including isopropylmalate dehydrogenases and tartrate dehydrogenases (Supplementary

Results, Supplementary Fig. 1). This alignment differed from a previous alignment of *HsIDH1* and the HIDHs that was based on primary sequence alone, which aligned *HsIDH1* Arg132 with a gap region in the other β -hydroxyacid oxidative decarboxylases⁸.

Using the alignment generated above, we identified and produced HIDH mutants that were analogous to human cancer-derived IDH mutants. Given that the enzymatic properties of wild type *Saccharomyces cerevisiae* (*Sc*) HIDH (65% amino acid identity with *Sp*HIDH) were well known^{10–12}, we chose to focus our efforts on producing and characterizing mutants of *Sc*HIDH. According to the new alignment and the structural overlay, *Sc*HIDH mutants R114Q, R143C, R143H, and R143K were analogous to the common cancer mutations IDH2-R140Q, IDH1-R132C, IDH1-R132H, and IDH2-R172K (Fig. 2b). These mutants as well as wild type *Sc*HIDH were produced and purified from bacteria (Supplementary Fig. 2).

To investigate whether one or more *Sc*HIDH mutants would convert 2-oxoadipate and NADH to (*R*)-2-hydroxyadipate and NAD⁺, specific activity was assessed by measuring the initial rate of NADH decrease catalyzed by the enzymes in reactions containing 2-oxoadipate and NADH. The R143C and R143H mutants, and to a lesser extent the R143K mutant, consumed NADH in a reaction containing 40 ng/ μ l enzyme, 10 mM 2-oxoadipate, and 300 μ M NADH, while no activity was observed for the R114Q mutant or for wild type *Sc*HIDH (Supplementary Fig. 3a). The rate of NADH decrease in the presence of the three Arg143 mutants increased hyperbolically with the concentration of 2-oxoadipate (Fig. 2c) and with the concentration of NADH (Supplementary Fig. 3b). The initial rate of NADH decrease was used to estimate kinetic parameters for the R143H mutant. For the R143H mutant, the substrate concentration for half maximal rate (K_M) for 2-oxoadipate was 2.0 ± 0.34 mM (s.d.) and the K_M for NADH was 85 ± 21 μ M (s.d.). These constants characterized *Sc*HIDH-R143H to have tight binding to NADH and moderate binding to 2-oxoadipate, comparable to the substrate-binding properties of the WT enzyme¹⁰. The maximal reaction rate (V_{max}) was 0.041 ± 0.0021 μ mol NADH $\text{min}^{-1} \text{mg}^{-1}$ (s.d.), which equates to a catalytic turnover rate (k_{cat}) of 1.6 min^{-1} . This rate is $\sim 1\%$ of the k_{cat} for WT *Sc*HIDH in the reductive direction¹⁰. No activity was observed when *Sc*HIDH-R143H was incubated with 15 mM of either 2-oxoglutarate or 2-oxoheptanedioate, indicating that *Sc*HIDH-R143H is specific for 2-oxoadipate and not other dicarboxylic acids (Supplementary Fig. 3c).

Next, the products of mutant *Sc*HIDH were investigated and compared to wild type *Sc*HIDH-WT. HIDH-WT normally carries out a reductive carboxylation reaction in which CO₂ is required as a substrate to carboxylate 2-oxoadipate and form homoisocitrate (see Fig. 1c, from right to left). When CO₂ was added to the reaction mix in the form of NaHCO₃, *Sc*HIDH-WT demonstrated 2-fold faster NADH consumption than *Sc*HIDH-R143H (Fig. 2d). In contrast to *Sc*HIDH-WT, *Sc*HIDH-R143H and -R143C activity was not stimulated by the addition of NaHCO₃. Liquid chromatography tandem mass spectrometry (LC-MS/MS) in negative electrospray ionization mode (-ESI) was undertaken to investigate the products of the wild type and R143H enzymes in the presence of 50 mM NaHCO₃ (Supplementary Fig. 4). [3,3,4,4]-²H₄-2-hydroxyglutarate was added to samples as an internal standard, and samples were derivatized with diacetyl-L-tartatic acid before binding to the HPLC column (see Supplementary Methods)^{20, 21}. Two Q1/Q3 transitions, each

representing a parent ion and a corresponding fragment ion, were monitored for the derivatives of homoisocitrate and of 2-hydroxyadipate. An intense homoisocitrate mass fragmentation pattern was observed in the reaction containing *ScHIDH*-WT (Q1/Q3 m/z = 421/205 and 421/187). In contrast, the *ScHIDH*-R143H reaction produced a 2-hydroxyadipate mass fragmentation pattern (Q1/Q3 m/z = 377/161 and 377/143). These results confirmed that *ScHIDH*-WT performs the expected reductive carboxylation of 2-oxoadipate to produce homoisocitrate and showed that *ScHIDH*-R143H catalyzes a non-carboxylating reductive reaction to produce 2-hydroxyadipate.

Since HIDHs are stereospecific for (*R*)-hydroxyacids as their substrates/products⁸, we predicted that the 2-hydroxyadipate produced by the *ScHIDH* mutants would be the (*R*) enantiomer of 2-hydroxyadipate. To confirm this, quantitative LC-MS/MS was performed using a 2-hydroxyadipate standard, and derivation with diacetyl-L-tartaric anhydride allowed the (*R*)- and (*S*)- enantiomers to be discriminated based on their elution time from the chiral HPLC column. (*R*)-2-hydroxyadipate stoichiometrically increased as NADH was consumed in reactions containing R143H, R143C, and R143K mutants (Supplementary Fig. 5). (*S*)-2-hydroxyadipate was undetectable in those reactions as shown in Fig. 2e. Even assuming that the (*S*) enantiomer was at the lower limit of quantification (0.84 μ M), these results indicated that the (*R*) enantiomer was produced in enantiomeric excess of >99.1% for the R143H mutant. This is consistent with the conversion of NADH, H⁺, and 2-oxoadipate to NAD⁺ and (*R*)-2-hydroxyadipate. Thus, *ScHIDH*-R143H, -R143C, and -R143K mutants are (*R*)-2-hydroxyadipate dehydrogenases.

We next investigated whether the new activity introduced by cancer-analogous mutations to *ScHIDH* was generalizable to an HIDH from a distantly related species, the thermophilic bacterium *Thermus thermophilus*⁹ (Supplementary Fig. 6). Arg118 of *TtHIDH* was analogous to Arg132 of *HsIDH1* based on structure-informed alignment. Interestingly, the WT enzyme from this species did display some HCO₃⁻-independent activity that resulted in stoichiometric (*R*)-2-hydroxyadipate production, though this activity was significantly increased in the *TtHIDH*-R118H mutant. However, unlike *ScHIDH*-R143H, *TtHIDH*-R118H consumed NADH at a 3-fold faster rate in the presence of 15mM 2-oxoglutarate than in the presence of 15mM 2-oxoadipate. Because of this substrate promiscuity, *TtHIDH*-R118H is likely not an ideal (*R*)-2-hydroxyadipate dehydrogenase for bio-based adipate production. Nevertheless, the finding that mutation of conserved residues conferred a change-of-function not only to *HsIDH1* and *HsIDH2*, but also to distantly related HIDHs, illuminated a conserved feature of the subfamily of β -hydroxyacid oxidative decarboxylases that act on (*R*)-hydroxy substrates to be redesigned into simple oxidoreductases.

We showed here that redesigned HIDH enzymes catalyze the novel NADH-dependent conversion of 2-oxoadipate to (*R*)-2-hydroxyadipate. These results defined a potentially generalizable rule that mutation of the arginine residues homologous to Arg132 of IDH1 (Arg143 of *ScHIDH*, Arg118 of *TtHIDH*) can introduce a change-of-function to enzymes of this subfamily. The redesigned enzymes had excellent enantioselectivity and moderate substrate binding properties. This establishment of desired activity for HIDH mutants represents first generation enzymes that can be further improved in catalytic turnover rate by directed evolution methods. The redesigned enzymes may be useful for bio-based adipic

acid production, for other metabolic engineering applications, and for the *in vitro* synthesis of chiral compounds. Metabolic enzymes running at high catalytic rates, such as malic enzyme and malate dehydrogenase, are known to produce off-target metabolites at low levels due to mechanistic promiscuity errors²². In a similar manner, IDHs catalyze off-target 2-hydroxyglutarate production at low levels²³. Active site IDH mutations in cancer alter substrate binding properties, structural conformational equilibrium, binding affinity for competitive inhibitors, and the rate of 2-hydroxyglutarate-producing catalysis to apparently favor 2-hydroxyglutarate production^{1, 23}. Though our approach to enzyme redesign was agnostic to chemical mechanism, the homology between HIDHs and IDHs suggests that analogous mechanistic changes are at work in the redesigned HIDH mutants.

Our strategy for enzyme redesign was to apply functional mutations observed in cancer cells to homologous enzymes. Though documented gain-of-function activities in metabolic enzymes resulting from cancer mutations are extremely rare so far, these results suggested that sequencing cancer genomes can provide a powerful source of functional mutation diversity to mine for additional novel enzyme activities. Even the numerous rarely-occurring mutations that are of marginal interest from a molecular pathology standpoint due to their rarity could still provide valuable insights for enzyme redesign. While computational design and directed evolution are certain to remain the major avenues to novel enzyme design, this study demonstrated that prospecting for alterations from human disease, and in particular cancer, can help to rapidly address a specific problem in enzyme design.

Supplementary Material

Refer to Web version on PubMed Central for supplementary material.

Acknowledgments

This work is supported by NIH grant R01 CA1403160 (H.Y.). We thank Paul F. Cook for an HIDH expression plasmid, Eric Spana for *S. cerevisiae* genomic DNA, Ping Fan for technical assistance, as well as Irwin Fridovich and Ines Batinic-Haberle for feedback on the manuscript.

Abbreviations

IDH	isocitrate dehydrogenase
HIDH	homoisocitrate dehydrogenase
Hs	Homo sapiens
Sp	Schizosaccharomyces pombe
Sc	Saccharomyces cerevisiae
Tt	Thermus thermophilus

References

1. Dang L, et al. Nature. 2009; 462:739–744. [PubMed: 19935646]
2. Niu W, Draths KM, Frost JW. Biotechnol Prog. 2002; 18:201–211. [PubMed: 11934286]

3. Noack H, Georgiev V, Blomberg MR, Siegbahn PE, Johansson AJ. *Inorg Chem.* 2011; 50:1194–1202. [PubMed: 21268602]
4. Sato K, Aoki M, Noyori R. *Science.* 1998; 281:1646–1647. [PubMed: 9733504]
5. Burgard, AP.; Pharkya, P.; Osterhout, RE. US patent. 2010/0330626. 2010.
6. Parthasarathy A, Pierik AJ, Kahnt J, Zelder O, Buckel W. *Biochemistry.* 2011; 50:3540–3550. [PubMed: 21434666]
7. Uhr ML, Thompson VW, Cleland WW. *J Biol Chem.* 1974; 249:2920–2927. [PubMed: 4151308]
8. Aktas DF, Cook PF. *Biochemistry.* 2009; 48:3565–3577. [PubMed: 19281248]
9. Miyazaki J, Kobashi N, Nishiyama M, Yamane H. *J Biol Chem.* 2003; 278:1864–1871. [PubMed: 12427751]
10. Lin Y, et al. *Biochemistry.* 2007; 46:890–898. [PubMed: 17223711]
11. Lin Y, et al. *Biochemistry.* 2008; 47:4169–4180. [PubMed: 18321070]
12. Lin Y, West AH, Cook PF. *Biochemistry.* 2009; 48:7305–7312. [PubMed: 19530703]
13. Chen R, Jeong SS. *Protein Sci.* 2000; 9:2344–2353. [PubMed: 11206056]
14. Parsons DW, et al. *Science.* 2008; 321:1807–1812. [PubMed: 18772396]
15. Mardis ER, et al. *N Engl J Med.* 2009; 361:1058–1066. [PubMed: 19657110]
16. Yan H, et al. *N Engl J Med.* 2009; 360:765–773. [PubMed: 19228619]
17. Ward PS, et al. *Cancer Cell.* 2010; 17:225–234. [PubMed: 20171147]
18. Xu X, et al. *J Biol Chem.* 2004; 279:33946–33957. [PubMed: 15173171]
19. Bulfer SL, Hendershot JM, Trievel RC. *Proteins.* 2012; 80:661–666. [PubMed: 22105743]
20. Struys EA, Jansen EE, Verhoeven NM, Jakobs C. *Clin Chem.* 2004; 50:1391–1395. [PubMed: 15166110]
21. Jin G, et al. *PLoS One.* 2011; 6:e16812. [PubMed: 21326614]
22. Kranendijk M, Struys EA, Salomons GS, Van der Knaap MS, Jakobs C. *J Inherit Metab Dis.* 2012; 35:571–587. [PubMed: 22391998]
23. Pietrak B, et al. *Biochemistry.* 2011; 50:4804–4812. [PubMed: 21524095]

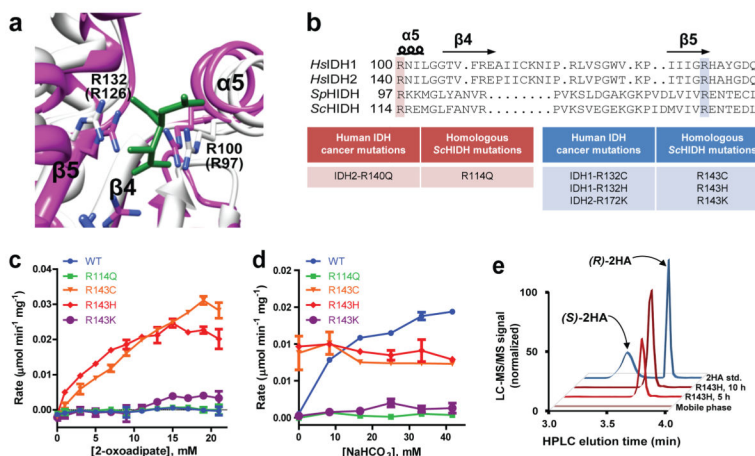


Figure 2. *ScHIDH* mutants catalyze the NADH-linked production of 2-hydroxyadipate
(a) Superimposition of the active site for *SpHIDH*¹⁹ (white) onto *HsIDH1*¹⁸ (pink; complex with isocitrate in green). Residues Arg100 and Arg132 of *HsIDH1* are shown, and corresponding residues for *SpHIDH* are shown in parentheses. **(b)** Alignment of *HsIDH1*, *HsIDH2*, *SpHIDH*, and *ScHIDH*. **(c)** Initial rate of NADH decrease catalyzed by the indicated *ScHIDH* mutant at varying concentrations of 2-oxoadipate, and 300 μ M NADH. **(d)** Initial rate of NADH decrease catalyzed by the indicated *ScHIDH* mutant in the presence of varying concentrations of NaHCO_3 , as well as 15 mM 2-oxoadipate and 100 μ M NADH. **(e)** LC-MS/MS chromatogram showing (*R*)-2-hydroxyadipate ($Q1/Q3$ $m/z = 377/161$) accumulation in a reaction containing *ScHIDH*-R143H, 2 mM NADH, 2 mM 2-oxoadipate, and 500 mM HEPES at times indicated. A racemic (*R/S*)-2-hydroxyadipate standard and mobile phase are shown for reference. Unless otherwise specified, all reactions contained 20 mM MgCl_2 , 40 ng/ μ l of the indicated purified enzyme, and 100 mM HEPES, pH 7.3. Data points are mean \pm s.d. from $n=2$ reactions. All plots are representative of three independent experiments.